

Can the variability in tropospheric OH be deduced from measurements of 1,1,1-trichloroethane (methyl chloroform)?

Maarten Krol and Jos Lelieveld

Institute for Marine and Atmospheric Research Utrecht, The Netherlands

Short title: OH VARIABILITY FROM METHYL CHLOROFORM MEASUREMENTS

Abstract.

Global three-dimensional model calculations have been used to inversely determine OH concentrations from 1,1,1-trichloroethane (methyl chloroform or MCF) measurements at the ALE/GAGE/AGAGE measurement stations. Annual global and bi-annual hemispheric estimates of OH show large fluctuations. With the aid of "pseudo data", it is shown that these estimates are sensitive to simplifying assumptions in the model that is used for the inversion. The use of climatological transport and errors in the emissions cause spurious fluctuations in the retrieved OH levels. If only the slow OH variations are considered, an OH increase of about 12% is calculated in the 1978–1990 period, which is followed by a slightly larger decline in the 1991–2000 period. The N/S inter-hemispheric ratio is optimized to a value of about 0.98, whereas the initial model calculated OH field has about 20% more OH on the northern hemisphere. The systematic differences between the results presented here and previous estimates can be explained by the more advanced transport model that is used in this study. Model calculations indicate that as a result of a rapidly decreasing MCF burden in the 1990s the stratospheric sink has become less important. Moreover, owing to the changed MCF distribution inter-hemispheric transport of MCF has ceased in recent years. These effects lead to systematic differences with results obtained with highly parameterized models with very low resolution. The large positive OH anomaly that is inferred around 1990 vanishes if MCF emissions of about 65 Gg are delayed from the early to the late 1990s. Recently observed large MCF variability over Europe suggests that such a delay has probably occurred, which would mean that global mean OH has been relatively constant over the past two decades.

1. Introduction

The hydroxyl radical (OH) plays an important role in the oxidation power of the troposphere. This short lived species with a lifetime of about 1 second initiates the breakdown of most hydrocarbons (CH_4 , CO and non-methane hydrocarbons (NMHC)). OH production is initiated by photolysis of ozone at ultraviolet (UV) wavelengths ($\lambda < 320 \text{ nm}$). The highly reactive oxygen atom that is formed in this photolysis, may react with water vapor to generate two OH radicals. Consequently, the highest OH concentrations are expected in the humid tropics where both water vapor and the UV light intensity maximize. Owing to the variability in tropospheric UV radiation, water vapor and ozone, the OH concentration in the troposphere is highly variable. *In-situ* measurements have confirmed this variability [e.g. *Mauldin et al.*, 2001], as well as the order of magnitude of the tropospheric concentration as estimated by chemistry transport models ($\approx 1 \times 10^6 \text{ molecules cm}^{-3}$, [WMO, 1999]).

Since the sources and sinks of OH vary considerably in space and time, *in-situ* measurements are generally not representative of the global average OH concentration. Such a global average can be obtained in an indirect way by observing species that are destroyed by OH. *Spivakovsky et al.* [2000] explored many of these species and indicated that 1,1,1 trichloroethane (methyl chloroform or MCF) is arguably the best species to constrain calculations of global tropospheric OH concentrations.

Since 1978, MCF has been measured at several stations that are evenly distributed over the globe. The Atmospheric Lifetime Experiment (ALE) was followed by the Global Atmospheric Gases Experiment (GAGE) and the Advanced Global Atmospheric Gases Experiment (AGAGE) [*Prinn et al.*, 2000]. Independently, *Montzka et al.* [2000] analyzed MCF flask samples that were collected at 7 to 10 remote locations.

The measurements show first of all that the atmospheric MCF concentrations have been declining since about 1992 as a consequence of the Montreal Protocol and its amendments. As a result, the atmospheric concentrations are currently lower than in 1978. The MCF increase up to 1992 and its subsequent decline has also been recorded in the accumulated ice sheets of Greenland and the South Pole [*Butler et al.*, 1999].

Secondly, the measurements reveal that the lowest mixing ratios are currently observed in the tropics. Since the emissions are now small compared to the atmospheric burden [Prinn *et al.*, 2001] this observation can only be explained by a relatively strong destruction by OH in the tropics. Thus, in addition to the global OH concentration, important information about the global OH distribution can be obtained from the MCF measurements [Spivakovsky *et al.*, 2000].

From the MCF decline in 1998 and 1999, Montzka *et al.* [2000] inferred a global MCF lifetime of about 5.2 years, which is somewhat longer than the estimate by Prinn *et al.* [2001] (4.9 years, estimated as burden divided by total loss) using the ALE/GAGE/AGAGE data. This latter estimate, however, represents an average over the entire 1978–2000 period. Prinn *et al.* [2001] furthermore inferred a global OH increase during the 1980s followed by an even stronger decrease in the 1990s. As a result, the inferred OH levels in 1998 and 1999 are lower than the 1978–2000 average.

In our earlier work [Krol *et al.*, 1998] (K98) we derived a positive 1978–1992 OH trend of about 0.5 \% year^{-1} using the ALE/GAGE measurements. This work was criticized by Prinn and Huang [2001] who obtained essentially a zero trend using a slightly longer time series (1978–1993) [Prinn *et al.*, 1995]. In a lengthy discussion it became clear that the difference was primarily caused by differences in the 1970–1978 emissions [Prinn and Huang, 2001; Krol *et al.*, 2001]. Whereas we optimized our initial condition, Prinn *et al.* [1995] used one specific emissions scenario. The fact that their recent analysis also reveals a positive OH trend in the 1980s reflects the different emissions that were used in later work [Prinn *et al.*, 2001]. A small modification in the absolute calibration of the measurements also slightly increased the inferred OH trend over this period.

The recent analysis of the entire 1978–2000 ALE/GAGE/AGAGE MCF record [Prinn *et al.*, 2001] revealed rapidly dropping OH levels in the 1990s. The estimated OH concentration in 2000 appeared to be $10 \pm 22\%$ lower than the 1979 values. Moreover, Prinn *et al.* [2001] inferred that OH concentrations in the Southern Hemisphere (SH) were on average $15 \pm 35\%$ lower than those in the Northern Hemisphere (NH). These

latter values are in good agreement with the independent estimate of *Montzka et al.* [2000]. Although the error margins are large, *Prinn et al.* [2001] conclude that there are "important and unexpected gaps in our understanding of the capability of the atmosphere to cleanse itself".

Chemistry transport models can alternatively be used to simulate the OH distribution and the associated change in time. When pre-industrial model calculations are compared to simulations of the modern atmosphere, most models predict a small reduction in tropospheric OH. For instance, *Wang and Jacob* [1998] calculated an OH reduction of only 9%, despite the fact that methane and CO concentrations increased by much higher percentages. Models that focused on the changing emissions during the recent decades sometimes simulate a small positive trend [*Karlsdóttir and Isaksen*, 2000; *Dentener et al.*, 2002]. From the model simulations it appears that the tropospheric OH abundance is quite efficiently buffered, i.e. stable to large perturbations [*Lelieveld et al.*, 2002]. To validate the modeled OH changes, independent estimates of the OH trend using MCF inversions are extremely valuable [*Singh*, 1977; *Prinn et al.*, 1995, 2001; *Krol et al.*, 1998]. In this work, the 1978–2000 ALE/GAGE/AGAGE MCF measurements are used to infer tropospheric OH concentrations with a 3D atmospheric model. We emphasize the ability of the inverse approach to obtain spatial and temporal variations in OH and the role of model errors, giving rise to caution for over-interpretation of MCF analyses.

2. Method

2.1. Inverse method

The inverse problem that is considered here can be written as:

$$\chi_{s,t} = F(\mathbf{P}, \mathbf{b}) + \sigma_{s,t}. \quad (1)$$

Here, $\chi_{s,t}$ and $\sigma_{s,t}$ (pmol/mol) denote time-series of the measured monthly mean MCF concentrations and corresponding standard deviations at the five ALE/GAGE/AGAGE stations; $F(\mathbf{P}, \mathbf{b})$ denotes the model simulated MCF at the stations. These values depend on the state vector \mathbf{P} and on other parameters that are collected in vector \mathbf{b} . To optimize the OH temporal or spatial variations, parameters that are linked to these variations

are included in the state vector. The other parameters, e.g. those linked to transport, emissions, and MCF destruction in the stratosphere and oceans, are included in \mathbf{b} .

The optimization of the parameters in the state vector is based on minimization of the cost function, which is defined as:

$$J(\epsilon, \mathbf{P}) = \frac{1}{2} \sum_{s=1}^5 \sum_{t=1}^{t_{max,s}} \frac{(\chi_{s,t} - \frac{1}{\epsilon} F(\mathbf{P}, \mathbf{b}))^2}{\sigma_{s,t}^2} + \frac{\Lambda}{2} \left(\frac{(\epsilon - \epsilon_{ap})^2}{\sigma_{\epsilon}^2} + \sum_{p=1}^{n_p} \frac{(P_p - P_{ap,p})^2}{\sigma_{P_p}^2} \right), \quad (2)$$

where ϵ is the absolute measurement calibration; vector \mathbf{P} refers to n_p free model parameters; Λ scales the *a priori* information given by ϵ_{ap} and P_{ap} with standard deviations σ_{ϵ} and $\sigma_{\mathbf{P}}$. Note that the absolute measurement calibration is always optimized along with the parameters in the state vector \mathbf{P} .

The first term of equation 2 sums the squared differences between model and measurements, weighted with the measured standard deviation during a month. Owing to declining emissions in the 1990s, these standard deviations have substantially reduced since the 1980s. The current approach does not use polynomial fitting like in K98. These polynomials filter out seasonal and interannual variability. One reason to use polynomial fitting was the inability of our climatological model to simulate interannual variability. However, the extension of the ALE/GAGE measurements with the AGAGE data hamper the use of low order polynomials. Moreover, when polynomials are used, the weighting at the beginning and the end of the time series might be slightly different compared to the original data [Prinn and Huang, 2001]. Although we showed that the derived OH trend and concentration are not influenced by the use of polynomials [Krol *et al.*, 2001], we decided to use the monthly averages and standard deviations directly in the optimization. Since the model uses monthly averaged winds, pollution events are excluded from the measurements [Prinn *et al.*, 2000].

Differences between model and measurements are caused by inaccuracies in the model transport, the applied MCF emissions, the OH distribution and its temporal variation, other MCF sinks (stratosphere, oceanic sink), MCF measurement calibration and chemical rate constants. Moreover, representation errors occur because point measurements are compared to large grid boxes in the model. It is assumed that the variations in the mixing ratios during a month ($\sigma_{s,t}$, pollution events excluded) provide

an estimate for these representation errors [Prinn *et al.*, 2001].

In the period 1978–2000 1248 (N) monthly averaged MCF concentrations at the ALE/GAGE/AGAGE stations are publically available (http://cdiac.ornl.gov/ftp/ale_gage_Agage/). An average deviation between model and measurements smaller than 1σ is considered to be a good fit and corresponds to a cost function value of about 1200 ($J/N \approx 1$).

The second term in equation 2 represents the costs related to deviations from the *a priori* information. The use of *a priori* information has two well known advantages [see e.g. Tarantola, 1987]: (i) the optimized parameters are constrained to values that are physically realistic, and (ii) the solution is stabilized. An unstable solution may occur if a parameter in the state vector is strongly correlated to other parameters. In that case, a range of parameter values corresponds to the same minimum of the cost function. *A priori* information of one or more parameters helps to avoid this, because the dependent parameter will then optimize to its *a priori* value. Correlations between the *a posteriori* determined parameters can be inferred from the co-variance matrix.

Since the number of observations is much larger than the number of unknowns in the current inversion, a factor Λ is introduced to scale the *a priori* information in the cost function. Without this factor, estimated parameters can deviate a few standard deviations from the *a priori* information without contributing significantly to the cost function. Introduction of $\Lambda = 100$ guarantees that, in this inverse problem, the free parameters are optimized well within their σ_{ap} values. Parameters that are not constrained by *a priori* information are given large σ_{ap} values. On the other hand, small σ_{ap} values can be used to constrain a parameter to a predefined value. No *a priori* constraints are placed on parameters that are related to OH. The absolute calibration uncertainty σ_ϵ is set to 5% [Prinn *et al.*, 2001] and whenever emissions are estimated, the associated 1σ uncertainty is used as an *a priori* constraint.

The cost function is minimized by varying the state vector \mathbf{P} until a minimum is obtained. Practically, the model is linearized around a solution \mathbf{P}_0 :

$$F(\mathbf{P}) = F(\mathbf{P}_0) + \frac{\partial F(\mathbf{P}_0)}{\partial \mathbf{P}} (\mathbf{P} - \mathbf{P}_0). \quad (3)$$

After minimization of the cost function (Equation 2) \mathbf{P}_0 is replaced by the new solution

and the procedure is repeated until convergence is reached. Owing to the linear nature of the perturbations, convergence is usually obtained in one iteration. The error covariance matrix of the estimated state vector is obtained from the linearized model, the measurement errors, and the *a priori* errors in the state vector [Tarantola, 1987]. It is assumed that the measurement errors are uncorrelated and Gaussian. The same assumptions apply to the *a priori* errors.

The procedure outlined here leads to results that are identical to our earlier approach which employed an ensemble smoother [Krol *et al.*, 1998], but is computationally more efficient. Additionally, the absolute calibration ϵ of the measurements is now optimized along with the other parameters in the state vector.

2.2. Model description

Two models have been used to perform the MCF simulations. The TM3 model [Dentener *et al.*, 1999; Lelieveld and Dentener, 2000; Peters *et al.*, 2001] is employed to perform simulations using 6-hourly analyzed wind fields from the European Centre for Medium range Weather Forecasts (ECMWF). The TM3 model is operated with a relatively coarse horizontal resolution of 7.5° latitude and 10° longitude and with 19 layers in the vertical. The upper five layers represent the stratosphere in which, apart from OH oxidation, photolysis of MCF is important. Photolysis rates in the stratosphere are calculated using a look-up table approach. The DISORT model [?] has been used to construct the look-up table. Cross-sections and quantum yield are taken from [DeMore W. B., *et al.*, 1997]. Monthly averaged OH fields as calculated for the year 1986 are used to oxidize MCF [Lelieveld and Dentener, 2000]. The 1986 meteorological fields are used in all years of the 1951–2000 simulation period.

The calculated lifetime for stratospheric loss (total atmospheric burden over stratospheric loss) calculated by TM3 amounts to about 45 years, in excellent agreement with other work [WMO, 1999]. The corresponding stratospheric loss rate (0–100 hPa burden over 0–100 hPa loss) amounts to about 2.5 year. Two reasons hamper the use of the TM3 model for MCF inversions: (i) the TM3 model is computationally too

expensive, and (ii) owing to the more detailed meteorology in TM3, pollution events will be partly resolved. A full simulation of all the pollution events, e.g. at the Ireland station [Ryall *et al.*, 2001] would require all years of meteorological data and a higher resolution of the model. Therefore, the TM3 simulations are used to tune the stratospheric loss in the MOGUNTIA model and to check the MCF budget (see Appendix).

As in K98 the MOGUNTIA model is used in the inversion of the MCF observations. The replacement of the Oregon station (45°N) by the California station (41°N) does not change the sampled grid box in the MOGUNTIA model. In MOGUNTIA, monthly averaged wind fields of the year 1986 are used to transport MCF. Emissions have been adapted from *McCulloch and Midgley* [2001] and the spatial distribution is similar to K98. For the recent years the emissions are distributed as in *Prinn et al.* [2001].

In K98 we accounted for the stratospheric sink by applying hemispheric mean and monthly varying loss rates at 100 hPa (the top of the model). Before 1990, MCF emissions increased continuously and caused a large concentration difference between the troposphere and the stratosphere. However, the emissions declined strongly in the 1990s and it is therefore expected that during this period the stratosphere becomes a less important sink for troposphere MCF. For this reason, we modified the stratospheric loss parameterization. Two reservoirs which represent the stratosphere (0–100 hPa) in the NH and the SH are added on top of the MOGUNTIA model. Exchange between the stratospheric reservoir and the upper model layer is calculated from the concentration difference multiplied by an exchange rate. The SH exchange rate is taken 33% slower than the NH value. The exchange rate and the stratospheric MCF lifetime are obtained from a simulation with the TM3 model as described previously. A more detailed discussion of the stratospheric parameterization is given in appendix A.

Uptake and subsequent hydrolysis of MCF in ocean water is modeled by a first order loss process [Krol *et al.*, 1998; Kanakidou *et al.*, 1995; Kindler *et al.*, 1995]. The loss rate is based on measurements reported by *Butler et al.* [1991], who observed negative saturation anomalies in the tropical pacific ocean in 1990. Hydrolysis of MCF is most efficient in warm ocean waters but MCF is much more soluble in the colder oceans at

higher latitudes. Hydrolysis in these waters proceeds much slower owing to the lower temperatures. Hydrolysis in cold oceans [Gerken and Franklin, 1989] is expected to be even slower than the observed atmospheric decay time since 1992. Cold oceans may therefore have acted as a buffer for the atmosphere since dissolved MCF may have been returned to the atmosphere. This idea is highly speculative and not tested while biological degradation in the productive waters at high latitudes can not be ruled out [Butler *et al.*, 1991]. Possible consequences for the MCF inversion, which appear to be small, are discussed in appendix B.

3. Annual and Hemispheric OH optimization

Following Prinn *et al.* [2001], we optimized 23 yearly and global OH scaling factors (1978–2000). These scaling factors are multiplied to our reference OH field [Krol *et al.*, 1998]. Simulations are performed from 1951 to 2000 and the 1978 scaling factor applies to all years before 1978 as well. In K98, the initial condition was also optimized. In the inversion of annual OH levels, however, optimization of the initial condition is no longer necessary because an increase in the pre-1978 emissions has the same effect on the cost function (Equation 2) as a decrease in the pre-1978 OH level. As a consequence, the optimization of both pre-1978 OH and pre-1978 emissions simply returns the *a priori* information for the emissions.

In addition to the optimization of global OH scaling factors, we also determined hemispheric OH scaling factors. These scaling factors are optimized in 2-yearly periods, which leads to a state vector length of 24. In our reference OH distribution, the OH concentration (weighted with the MCF+OH reaction rate [Lawrence *et al.*, 2001]) in the NH exceeds the SH value by about 20%.

The results of the optimizations are shown in Figure 1. The values for ϵ are 0.989 ± 0.003 and 0.996 ± 0.005 for the global and hemispheric OH optimizations, respectively (reported errors from inversion only). The optimized J/N values are 0.77 and 0.60, respectively. With an average deviation well within the 1σ level, the optimized model results are in excellent agreement with the ALE/GAGE/AGAGE measurements.

Figure 1

Hemispheric OH optimization gives an even better fit to the measurements than the global OH optimization.

Similar to the results of *Prinn et al.* [2001] the optimized OH levels show large fluctuations. Year to year jumps of more than 10% in hemispheric and global OH concentrations are not uncommon. Are these temporal and spatial variations real, or are they associated with the estimation method? In the following we will show that these variations are most likely an artifact of the method.

4. Analysis of the OH fluctuations

An important aspect to consider in the inversion is the atmospheric lifetime of MCF (about 5 years). It exceeds the mixing time in the troposphere and is also large compared to the temporal variations in the retrieved OH. By fixing all parameters b in Equation 1 it is implicitly assumed that all discrepancies between model and measurement are explained by variations in OH. This means that errors in b (transport, other sinks, etc.) are potentially translated in OH variations during the inversion process. As an example, the derived declines in global OH during El Niño Southern Oscillation (ENSO) events might be real, but might also be caused by the fact that the model does not account for interannual transport variability [*Prinn et al.*, 2001].

Another possible cause for the retrieved OH fluctuations might be the ill-posed nature of the inversion itself. This situation occurs when parameters become redundant and do not longer reduce the value of the cost function. Ill-posed inversions can be stabilized by applying some kind of regularization, such as providing *a priori* information or, alternatively, a smoothness constraint [e.g. *Hasekamp and Landgraf*, 2001].

The possibility of an ill-posed inversion is investigated by replacing the ALE/GAGE/AGAGE measurements with "pseudo data" that are calculated by the model itself. We prescribed a linear OH trend (-6% in 1978 to $+5\%$ in 2000, relative to the reference field) to the model. The adopted 1σ errors of the pseudo data are identical to the ALE/GAGE/AGAGE measurements. The pseudo data are perturbed with small random noise. If the inversion procedure is applied to these data, we indeed retrieve the

prescribed trend in OH (see Figure 2a). Therefore, the inversion itself is not ill-posed.

Figure 2

This leaves the possibility that the retrieved OH fluctuations are caused by model errors. Therefore, the inversion of the model generated pseudo data is repeated, but now with slightly modified model formulations. To account for uncertainties in the model transport we performed two simulations with the more advanced transport model TM3. In one simulation the 1986 meteorological data are used for all years in the 1951-2000 period. In the second simulation, the meteorology of the years 1979-1997 is used for the corresponding years. As an example, Figure 3 shows the ratio of the monthly mean concentrations in these two simulations as sampled in the Barbados grid box.

Figure 3

Obviously, transport alone generates interannual variability of the order of a few percent in the simulated concentrations, even when it is monthly averaged. The calculated ratio of the two simulations is used to estimate the magnitude of the interannual transport variability at the stations. To test the influence on the OH inversion, we multiplied this ratio evaluated at the five ALE/GAGE/AGAGE stations to the pseudo measurements, and repeated the inversion. The result is included in Figure 2a (dotted line). Also included are the inversion results of simulations in which (i) the emissions were randomly varied within their 1σ uncertainties (dash-dotted), and (ii) the convective fluxes in the model were multiplied by a factor 0.5 (dashed).

Clearly, the calculated yearly OH concentrations are very sensitive to errors in meteorology and MCF emissions. Global deviations from the true solution may be as large as 7%, for example in 1994 and 1998. Moreover, changing the convective fluxes results in systematic deviations. However, the linear trend in the true solution can still be inferred from all results. It can thus be concluded that the inversion of OH scaling factors for single years is very sensitive to modeling errors and that only variations on the longer time scales can be inferred from MCF inversions.

The fact that OH concentrations can only be retrieved as long-term means implies that the retrieval of hemispheric OH values will also be sensitive to model errors, since inter-hemispheric transport times are in the order of 1 year. To show this sensitivity, we repeated the inversion of pseudo data, prescribing a positive OH trend in the NH and a

negative trend in the SH. We inverted 2-year OH averages in the NH and the SH, using the different model versions described earlier. The results are summarized in Figures 2b and 2c. Again, some skill in inverting the prescribed OH trend in the hemispheres seems to be present. However, the deviations become particularly large in the inversion with modified transport. For instance, the large negative OH deviations in the NH are partly compensated by positive deviations in the SH. These correlations are quantified in the covariance matrix. Correlation coefficients between the bi-annual OH estimates of the hemispheres range from -0.68 to -0.98 .

From these experiments with pseudo data it can be concluded that the large OH fluctuations that are retrieved from the global annual and hemispheric bi-annual OH inversions are probably caused by modeling errors. A similar observation was made by [Houweling *et al.*, 1999] who optimized methane emissions from a surface measurement network. Our results indicate that some information about OH variations on the slower time scale can be retrieved as long as model errors are not too large. Therefore, the inversion of the ALE/GAGE/AGAGE data is only meaningful by focusing on these slower OH variations.

5. OH changes on a long time scale

The OH levels are now estimated in 3 and 5 year periods. These periods are sufficiently long to smooth the effects of the errors in emissions and meteorology, at least the random part of these errors. In addition, the OH change in time has been expressed as a second order polynomial [Prinn *et al.*, 2001]:

$$OH(t) = OH(ref) \left(1 + \frac{a}{100} \right) \left(1 + \frac{b}{100} NP_1\left(\frac{t}{N} - 1\right) + \frac{c}{300} N^2 P_2\left(\frac{t}{N} - 1\right) \right), \quad (4)$$

in which N amounts to 11 year and t runs from 0 (1978) to $2N$ (2000) and P_1 and P_2 are Legendre polynomials. a (%), b (% yr $^{-1}$), and c (% yr $^{-2}$) are included in the state vector. Alternatively, coefficient a is determined for the NH and SH separately, to estimate the time-averaged N/S inter-hemispheric ratio. In the inversions, the 1970–1978 emissions are also optimized by determining a single factor that is multiplied to the yearly emissions in this period. The *a priori* error for this factor is assumed to be 2%.

The results are summarized in Figure 4, 5 and Tables 1–4. Figure 5 shows the modeled and observed e-fold decay times calculated from monthly means at the end of each yearly period as e.g. $\tau_{2000.5} = (\ln\chi_{2000.5} - \ln\chi_{1999.5})^{-1}$ [Montzka *et al.*, 2000]. The results have been obtained with OH variation optimized according to Eq. 4. The average e-fold decay time calculated from the AGAGE data and from our model (about 5.7 years) is slightly slower than the decay time deduced by Montzka *et al.* [2000]. Note that the remaining discrepancies between model and measurements may be explained by OH variations on both hemispheres. However, we have shown above that model errors or uncertainties in the MCF emissions are a more plausible explanation. The resulting correspondence between the model and the measurements is very good, considering possible model errors and emission uncertainties.

With regard to the deduced variations in OH, the results confirm the results obtained by [Prinn *et al.*, 2001] with a few exceptions. Their optimized polynomial yields 15% lower OH levels in 2000 compared to the levels in 1978. This lower OH level has been interpreted as a possible collapse of the oxidizing capacity of the troposphere. In contrast, our optimization leads to OH levels in 2000 which are only slightly lower than the pre-1980 levels. The N/S hemispheric OH ratio optimized in our model (see Table 4) amounts to 0.98, which also differs from the ratio of 0.88 presented by Prinn *et al.* [2001] ($14 \pm 35\%$ more OH in the SH). Nevertheless, these results appear to confirm that the MCF measurements point to a significant increase in OH levels during the 1980s and a subsequent decline in the 1990s.

6. Discussion

Although the results presented here fall well within the wide error margins given by Prinn *et al.* [2001] the N/S hemispheric ratio and the OH decline in the late 1990s differ systematically. These differences can be understood from model differences. A very low-resolution model has limited ability to simulate the effects of the changing MCF distribution on inter-hemispheric MCF transport and on MCF exchange between the troposphere and stratosphere. For instance, the transport in the model used by Prinn

Figure 4, 5

Tables 1–4

et al. [2001] has been tuned to observations of F11 and F12. However, these tracers behave distinctly different from MCF, which has an important tropospheric sink. The N/S inter-hemispheric OH ratio of 0.88 as calculated by *Montzka et al.* [2000] is based on a two-box budget approach. This approach assumes that inter-hemispheric transport is proportional to the inter-hemispheric concentration difference.

Our model results indicate that the inter-hemispheric exchange in the late 1990s becomes negligible with equal amounts of OH in both hemispheres. Since the major MCF sink is located in the tropics, transport of MCF in recent years occurs mainly between the high and low latitudes within both hemispheres. To model small inter-hemispheric transport of MCF in the presence of a large OH gradient requires a higher resolution than is provided by two or four boxes. The same argument applies to the stratosphere–troposphere exchange. Although the stratosphere in the MOGUNTIA model is also very simple, it has been tuned to a model that explicitly resolves the stratosphere (see Appendix A).

The fact that we estimate more OH on the Southern Hemisphere (in apparent conflict with our model calculations) might well be due to model errors as discussed above. For instance, additional emissions of 30 Gg yr^{-1} over Europe in the period 1998–2000 requires 12% higher 1998–2000 global OH levels to remain consistent with the measurements. Moreover, such an additional source would change the optimized N/S inter-hemispheric ratio from 0.98 into 1.06. Unexpected MCF emissions in recent years likely occur in Europe and possibly other regions, as indicated by MCF measurements in 2000 and 2001, showing much higher concentrations and variability than expected from the emissions that are used in the inversions (Krol *et al.*, Evidence for substantial 1,1,1-trichloroethane emissions from Europe, submitted manuscript).

Another important factor is that the mean location of the Inter-Tropical Convergence Zone (ITCZ) is at 6°N [*Waliser and Gautier*, 1993], so that the average SH air mass is approximately 12% larger than the NH from the viewpoint of inter-hemispheric mixing. Since OH is concentrated in the tropics, the "division" between the two hemispheres strongly influences the inter-hemispheric OH ratio calculations from MCF distributions,

notably for the period when MCF concentrations were substantially higher in the NH. The apparent discrepancy between the MCF derived OH asymmetry and that calculated by chemistry-transport models, may therefore be an artifact from the assumption that the meteorological hemispheres are symmetrical around the equator. Improved estimates of inter-hemispheric OH differences from MCF analyses therefore await inversion models that properly resolve the ITCZ. The fact that our inversion model (10° resolution) calculates a significantly higher NH/SH interhemispheric ratio than models with an even lower resolution, points to a high sensitivity of this ratio for the model resolution.

To show which emissions correspond to a time-invariant OH burden, the global MCF source can be optimized assuming constant OH levels [Prinn *et al.*, 2001]. Thus we scaled our reference OH field by -7.4% (according to Table 3 and Eq. 4), and estimated the emissions in three-year periods. As for OH, emission scaling factors have been determined without taking any *a priori* information into account. Note that this approach does not maintain constant total emissions (a quantity that can be estimated relatively accurately).

The results, summarized in Table 5, indicate that a shift in emissions of about 100–150 Gg from the 1983–1991 period to the pre-1983 and post-1991 periods would be required to arrive at a constant OH level. Such a shift represents a relatively small amount of the emissions that occurred in the early 1990s, but is large compared to the emission estimates for the recent years. A relatively small error in the banking time to the "slow-use" category [Midgley and McCulloch, 1995; McCulloch and Midgley, 2001] during the early 1990s is required to explain the AGAGE measurements in the recent years without a significant drop in OH. Note also that the optimization of the emissions results in a slightly better fit to the observations ($J/N \approx 0.9$) than the optimization of OH ($J/N \approx 1.0$, see Table 1).

Table 5

Based on calculations using chemistry transport models, large interdecadal swings in global tropospheric OH concentrations are not expected. For instance, the methane growth rate varied from about 20 ppbv yr^{-1} in the 1970s and 12 ppbv yr^{-1} in the 1980s, to almost zero in 1992–1993 [Lelieveld *et al.*, 1998; Dlugokencky *et al.*, 1998]. It is

unlikely, however, that OH level changes are the sole cause of the decline in the methane growth rate in the early 1990s. More likely, the natural wetland emissions temporarily declined after the Mt. Pinatubo eruption [*Hogan and Harriss*, 1994; *Walter et al.*, 2001; *Dentener et al.*, 2002]. Positive methane growth rates were restored after 1993, whereby variability has been attributed to the variability in emissions [*Dlugokencky et al.*, 2001].

Model calculations that focused on the 1979-1993 period point to a small increase in OH of about 0.25 \% yr^{-1} during this period [*Dentener et al.*, 2002]. This increase can partly be attributed to changes in stratospheric ozone, OH precursor emission changes, and meteorological variability. Meteorological variability alone causes year-to-year changes in the global tropospheric OH burden of a few percent. This variability might become somewhat larger if also the full variability in emissions (e.g. from biomass burning) would have been taken into account. From these model calculations it appears, however, that interdecadal variability of more than 10% is in contradiction with observed methane growth rates.

In fact, the remarkable co-variation of the global MCF burden and the optimized OH variations (with maximum OH levels in the late 1990s), both in our results and even more strongly in those by *Prinn et al.* [2001], signals a systematic modeling error. If the recent MCF emissions over Europe are indeed much higher than estimated, this points to a shift in emissions from the early early 1990s to the recent years, understandable in the light of enhanced stockpiling associated with the phase-out of MCF production under the Montreal Protocol. Such a shift in emissions would leave the total emission (i.e. a quantity that can be estimated relatively accurate) unaffected. It would also lead to much smaller interdecadal OH variations, which in turn is more consistent with observed methane growth rates and atmospheric chemistry modeling [*Lelieveld et al.*, 2002; *Dentener et al.*, 2002].

7. Conclusions

Using a 3D global transport model, variations in tropospheric OH have been determined from MCF measurements at the ALE/GAGE/AGAGE stations. The main

conclusions are:

- Inter-annual global and hemispheric OH inversions are very sensitive to modelling errors, in particular of the MCF emission estimates.
- Inverse OH retrieval techniques based on MCF observations are not suited to accurately infer short-term OH variability (>3 years), unless highly accurate models are used that resolve actual meteorology. Provided that MCF emissions are known accurately, these techniques are adequate to study long-term OH changes.
- Estimates of the slow and large scale OH variations indicate a substantial increase ($\approx 12\%$) in the 1978–1990 period, followed by a slightly larger decrease in the decade 1991–2000. Hence the overall trend over the entire period is close to zero.
- The calculated MCF decline depends relatively strongly on the changes of the stratospheric MCF sink. Owing to the fast decline of tropospheric MCF and a "buffering" effect, this sink has become substantially less important in the recent years.
- The large swings of OH on interdecadal time scales are in conflict with observed methane growth rates and with model calculations. A shift in emissions from the early 1990s to the recent years offers a plausible explanation to both the observed decline in atmospheric MCF and the MCF variability observed over Europe during 2000 and 2001.
- The question of inter-hemispheric OH (a)symmetry will remain unresolved until MCF emissions are quantified with higher accuracy, and until MCF transport models are used that resolve the ITCZ and adequately describe inter-hemispheric exchange. Our results indicate a small inter-hemispheric OH difference.

Definite conclusions about the trend in tropospheric OH cannot be drawn before the quantitative understanding of the MCF emissions is improved. Measurements that aim at the localization of possible ongoing MCF emissions are therefore urgently required.

Appendix A: Stratospheric Loss

Time scales associated with stratospheric MCF loss are larger than the mixing time in the troposphere. Loss predominantly occurs by photolysis in the upper troposphere and therefore the turnover time (burden/loss) in the stratosphere is not only determined by chemistry, but also by transport. During the 1980s MCF emissions increased strongly and the stratospheric concentrations were relatively low compared to tropospheric concentrations. This situation changed in the late 1990s. Emissions dropped and, due to the time delay associated with stratospheric transport, the relative concentration difference between the stratosphere and troposphere decreased [Prather, 1998].

The TM3 model explicitly takes the stratospheric removal of MCF into account. Although one might argue that the vertical resolution in the upper stratosphere (levels at 10, 30 and 50 hPa) is not sufficient to model the MCF photolysis correctly, the estimated lifetime with respect to stratospheric loss agrees well with other estimates [WMO, 1999]. Table A1 lists the lifetimes as calculated in the TM3 and MOGUNTIA models, both operated with unscaled and constant OH fields. These lifetimes are defined as tropospheric burden over process loss [Prather, 1998]. The processes considered are (i) OH oxidation (ii) removal by ocean uptake and (iii) loss to the stratosphere. Note that the lifetimes are calculated for the tropospheric burden (1000–100 hPa), which results in smaller values compared to calculations that also include the stratospheric burden.

Although the results of the two models differ slightly, the tendencies are the same. The lifetime of the tropospheric burden with respect to stratospheric loss increases significantly from about 34 years to 58 years. As a result, the total tropospheric lifetime increases in both models by about 6%. Given the large differences between the TM3 and MOGUNTIA models it can be concluded that the simple parameterization outlined in Section 2 performs well.

Appendix B: Oceanic Removal

The time scale that is associated with hydrolysis of MCF in cold ocean water is longer than the atmospheric decay observed in the 1990s [Gerken and Franklin,

1989; *Butler et al.*, 1991]. For this reason, the cold ocean water may have become supersaturated relative to the atmosphere during the period of fast atmospheric decline. To estimate the effect of such a buffering effect on the OH inversion, the ocean sink parameterization was modified. Thus, the ocean mixed layer was treated as a well-mixed reservoir that is in equilibrium with the lower atmosphere. The MCF budget in the mixed layer is calculated by uptake or release to the atmosphere and a temperature dependent hydrolysis reaction [*Gerken and Franklin*, 1989]. Other terms, like horizontal transport and transport to the deep ocean have been neglected for simplicity. As in K98, monthly mean climatologies of the mixed layer temperature and thermocline depth were used.

By using this simple parameterization in the inversion, the 2000 OH level is calculated to be about 4% higher than with the first-order oceanic loss, which implies that the effect on the OH trend calculations is only small. At present, however, not enough measurements are available to validate the buffering effect of the cold oceans. Moreover, the effects of horizontal and vertical transport within the ocean has been neglected. For these reasons, and because the effect is calculated to be relatively small, oceanic removal was still treated as a first order loss process, as described in K98.

Acknowledgments. This research was supported by Space Research Organization Netherlands. M.K. is grateful for support from many colleagues. Otto Hasekamp and Jochen Landgraf are acknowledged for their insight in inverse problems; Sander Houweling and Frank Dentener for their stimulating discussions. R. Prinn and co-workers are acknowledged for the ALE/GAGE/AGAGE measurements.

References

References

- Butler, J., J. Elkins, T. Thompson, B. Hall, T. Swanson, and V. Koropalov, Oceanic consumption of CH_3CCl_3 : Implications for tropospheric OH, *J. Geophys. Res.*, *96*, 22,347–22,355, 1991.
- Butler, J. H., M. Battle, M. L. B. S. A., Montzka, A. D. Clarke, E. S. Saltzman, C. M. Sucher, J. P. Severinghaus, and J. W. Elkins, A record of atmospheric halocarbons during the twentieth century from polar firn, *Nature*, *399*, 749–755, 1999.
- DeMore W. B., et al., Chemical kinetics and photochemical data for use in stratospheric modelling, vol. JPL Publication 97-4. Jet Propulsion Laboratory, Pasadena, CA, 1997.
- Dentener, F., J. Feichter, and A. Jeuken, Simulation of the transport of Rn-222 using on-line and off-line global models at different horizontal resolutions: a detailed comparison with measurements, *Tellus*, *B51*, 573–602, 1999.
- Dentener, F., M. van Weele, M. Krol, S. Houweling, and P. van Velthoven, Trends and inter-annual variability of methane emissions derived from 1979-1993 global CTM simulations, *Atmos. Chem. Phys. Discus.*, *2*, 249–287, 2002.
- Dlugokencky, E. J., K. A. Masarie, P. M. Lang, and P. P. Tans, Continuing decline in the growth rate of the atmospheric methane burden, *Nature*, *393*, 447–450, 1998.
- Dlugokencky, E. J., B. P. W. and K. A. Masarie, P. M. Lang, and E. S. Kasischka, Measurements of an anomalous global methane increase during 1998, *Geophys. Res. Lett.*, *28*, 499–502, 2001.
- Gerken, R. R., and J. A. Franklin, The rate of degradation of 1,1,1 trichloroethane in water by hydrolysis and dechlorination, *Chemosphere*, *19*, 1929–1937, 1989.
- Hasekamp, O. P., and J. Landgraf, Ozone profile retrieval from backscattered ultraviolet radiances: The inverse problem solved by regularization, *J. Geophys. Res.*, *106*, 8077–8088, 2001.
- Hogan, K. B., and R. C. Harriss, A dramatic decrease in the growth-rate of atmospheric methane in the northern-hemisphere during 1992 - comment, *Geophys. Res. Lett.*, *21*, 2445–2446, 1994.
- Houweling, S., T. Kaminski, F. J. Dentener, J. Lelieveld, and M. Heimann, Inverse modeling of

- methane sources and sinks using the adjoint of a global transport model, *J. Geophys. Res.*, *104*, 26137–26160, 1999.
- Kanakidou, M., F. J. Dentener, and P. J. Crutzen, A global three-dimensional study of the fate of HCFCs and HFC-134a in the troposphere, *J. Geophys. Res.*, *100*, 18,781–18,801, 1995.
- Karlsdóttir, S., and I. S. A. Isaksen, Changing methane lifetime: Possible cause for reduced growth, *Geophys. Res. Lett.*, *27*, 93–97, 2000.
- Kindler, T. P., W. L. Chameides, P. H. Wine, D. M. Cunnold, F. N. Alyea, and J. A. Franklin, The fate of atmospheric phosgene and the stratospheric chlorine loadings of its parent compounds - CCL₄, C₂CL₄, CH₂CL₃, CH₃CCL₃, and CHCL₃, *J. Geophys. Res.*, *100*, 1235–1251, 1995.
- Krol, M. C., P. J. Van Leeuwen, and J. Lelieveld, Global OH trend inferred from methylchloroform measurements, *J. Geophys. Res.*, *103*, 10,697–10,711, 1998.
- Krol, M. C., P. J. Van Leeuwen, and J. Lelieveld, Comment on "Global OH trend inferred from methylchloroform measurements", by Maarten Krol et al. - Reply, *J. Geophys. Res.*, *106*, 23159–23164, 2001.
- Lawrence, M. G., P. Jöckel, and R. von Kuhlmann, What does the global mean oh concentration tell us?, *Atmos. Chem. Phys.*, *1*, 37–49, 2001.
- Lelieveld, J., and F. Dentener, What controls tropospheric ozone?, *J. Geophys. Res.*, *105*, 3531–3551, 2000.
- Lelieveld, J., P. J. Crutzen, and F. J. Dentener, Changing concentration, lifetime and climate forcing of atmospheric methane, *Tellus*, *B50*, 128–150, 1998.
- Lelieveld, J., W. Peters, F. J. Dentener, and M. Krol, Stability of tropospheric hydroxyl chemistry, *J. Geophys. Res.*, *107*, (submitted), 2002.
- Mauldin, R. L., et al., Measurements of OH aboard the NASA P-3 during PEM-Tropics B, *J. Geophys. Res.*, *106*, 32657–32666, 2001.
- McCulloch, A., and P. M. Midgley, The history of methyl chloroform emissions: 1951–2000, *Atmos. Environ.*, *35*, 5311–5319, 2001.
- Midgley, P., and A. McCulloch, The production and global distribution of emissions to

- the atmosphere of 1,1,1, trichloroethane (methyl chloroform), *Atmos. Environ.*, *29*, 1601–1608, 1995.
- Montzka, S. A., C. M. Spivakovsky, J. H. Butler, J. W. Elkins, L. T. Lock, and D. J. Mondeel, New observational constraints for atmospheric hydroxyl on global and hemispheric scales, *Science*, *288*, 500–503, 2000.
- Peters, W., M. Krol, F. Dentener, and J. Lelieveld, Identification of an El Niño-Southern Oscillation signal in a multiyear global simulation of tropospheric ozone, *J. Geophys. Res.*, *106*, 10389–10402, 2001.
- Prather, M. J., Timescales in atmospheric chemistry: CH₃Br, the ocean, and ozone depletion potentials, *Global Biochem. Cycles*, *11*, 393–400, 1998.
- Prinn, R. G., and J. Huang, Comment on "global OH trend inferred from methylchloroform measurements" by Maarten Krol et al., *J. Geophys. Res.*, *106*, 23151–23157, 2001.
- Prinn, R. G., R. F. Weiss, B. R. Miller, J. Huang, F. N. Alya, D. M. Cunnold, P. J. Fraser, D. E. Hartley, and P. G. Simmonds, Atmospheric trends and lifetime of CH₃CCl₃ and global OH concentrations, *Science*, *269*, 187–190, 1995.
- Prinn, R. G., et al., A history of chemically and radiatively important gases in air deduced from ALE/GAGE/AGAGE, *J. Geophys. Res.*, *105*, 17751–17792, 2000.
- Prinn, R. G., et al., Evidence for substantial variations of atmospheric hydroxyl radicals in the past two decades, *Science*, *229*, 1882–1888, 2001.
- Ryall, D. B., R. G. Derwent, A. J. Manning, P. G. Simmonds, and S. O'Doherty, Estimating source regions of European emissions of trace gases from observations at Mace Head, *Atmos. Environ.*, *35*, 2507–2523, 2001.
- Singh, H. B., HO concentrations in the northern and southern hemisphere, *Geophys. Res. Lett.*, *4*, 453–456, 1977.
- Spivakovsky, C. M., et al., Three-dimensional climatological distribution of tropospheric OH: Update and evaluation, *J. Geophys. Res.*, *105*, 8931–8980, 2000.
- Tarantola, A., *Inverse Problem Theory: Methods for Data Fitting and Model Parameter Estimation*. Elsevier, New York, 1987.

Waliser, D. E., and C. Gautier, A satellite derived climatology of the ITCZ, *J. Clim.*, *6*, 2162–2174, 1993.

Walter, B. P., M. Heimann, and E. Matthews, Modeling modern methane emissions from natural wetlands 1. model description and results, *J. Geophys. Res.*, *106*, 34189–34206, 2001.

Wang, Y. H., and D. J. Jacob, Anthropogenic forcing on tropospheric ozone and OH since preindustrial times, *J. Geophys. Res.*, *103*, 31123–31135, 1998.

WMO, Scientific assessment of ozone depletion: 1998, vol. 44. World Meteorological Organization, Geneva, Switzerland, 1999.

M. Krol and J. Lelieveld,

Institute for Marine and Atmospheric Research Utrecht,

Utrecht University, Princetonplein 5,

3584 CC, Utrecht, The Netherlands,

(e-mail: krol@phys.uu.nl;

lelieveld@mpch-mainz.mpg.de)

Received _____

Submitted to *J. Geophys. Res.*, , 2002.

This manuscript was prepared with AGU's \LaTeX macros v4, with the extension package 'AGU++' by P. W. Daly, version 1.5d from 1997/04/28.

Received _____

Submitted to *J. Geophys. Res.*, , 2002.

This manuscript was prepared with AGU's \LaTeX macros v4, with the extension package 'AGU++' by P. W. Daly, version 1.5d from 1997/04/28.

Figure 1.

Figure 2.

Figure 3.
Figure 4.

Figure 5.

Table 1.

Table 2.

Table 3.

Table 4.

Table 5.

Table 6.

Figure Captions

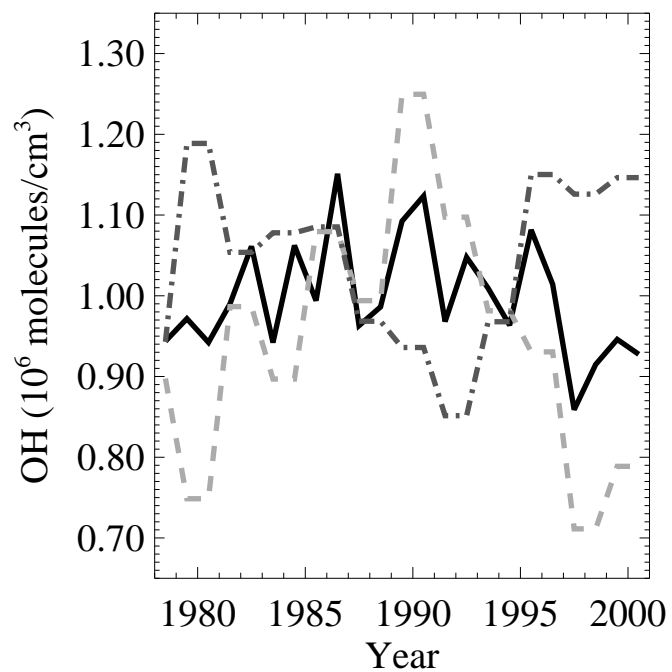


Figure 1. Estimated mass-weighted OH concentrations. Solid line: global; Light dashed line: NH; Grey dash-dotted line: SH

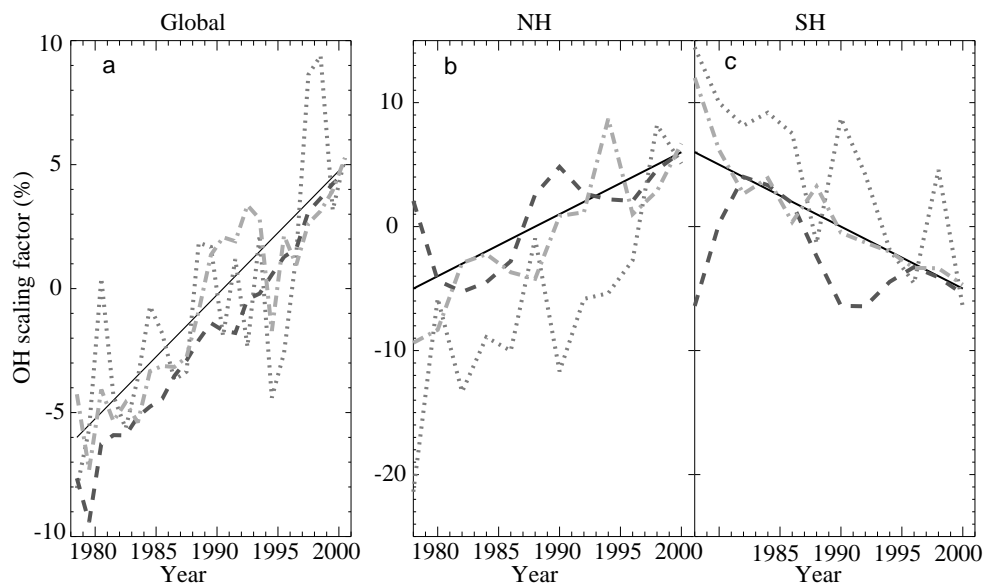


Figure 2. Inversion of pseudo data for (a) Global (b) NH, and (c) SH OH scaling factor. Solid thin lines: prescribed trend; Dotted lines: varying meteorology; Dashed lines: convection $\times 0.5$; Dot-dashed lines: perturbed emissions

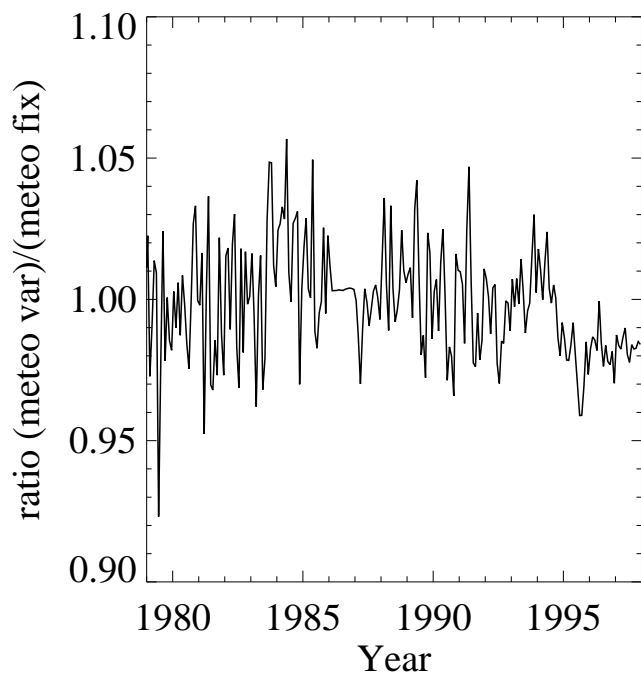


Figure 3. Ratio of the Barbados MCF concentration calculated with actual meteorology and with constant 1986 meteorology

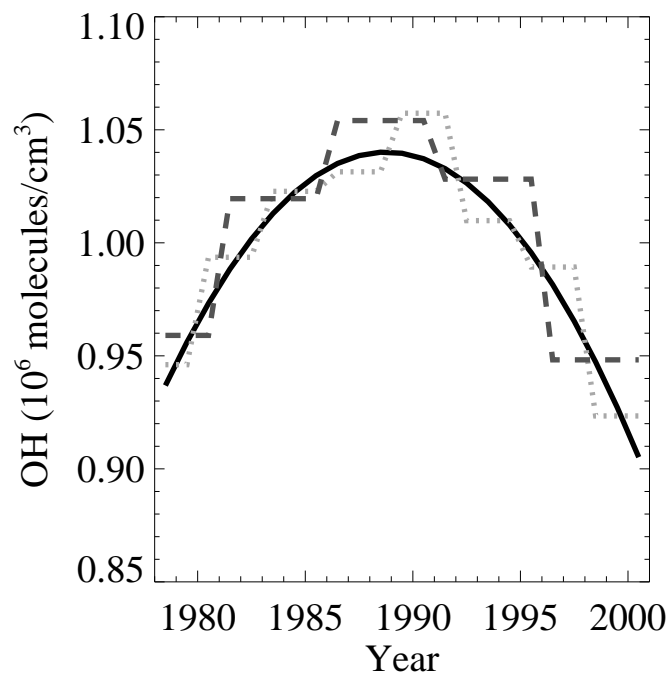


Figure 4. Trend calculated in 3 year periods (light dotted), 5 year periods (grey dashed), and using the polynomial of Eq. 4 (solid)

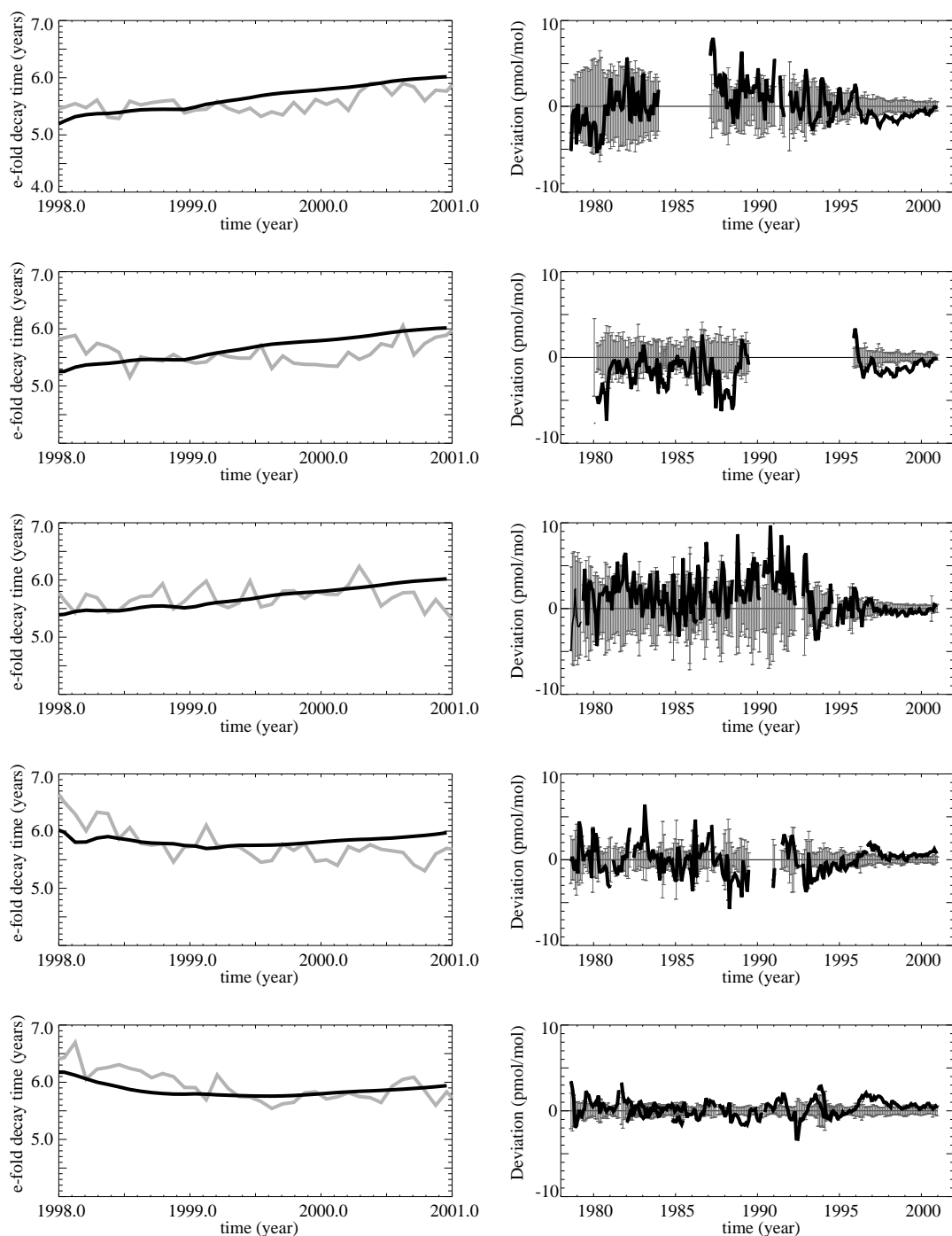


Figure 5. Left panels: 1998–2000 decay time calculated from the GAGE data (gray line) and from the model results with OH optimized using Eq. 4. Right panels: residual deviations between the measurements (grey bars, normalized to zero) and the optimized model (black lines). From top to bottom: Mace Head, Oregon/California, Barbados, Samoa, and Tasmania

Tables

Table 1. Optimization of OH in 3-Year Periods

Parameter	Value	σ^a
1951–1979 ^b	–12.4	0.7
1980–1982	–8.0	0.5
1983–1985	–5.3	0.5
1986–1988	–4.5	0.5
1989–1991	–2.1	0.5
1992–1994	–6.5	0.4
1995–1997	–8.4	0.2
1998–2000	–14.5	0.3
ΔE^c	0.0	0.2
ϵ	0.992	0.003
J/N	1.00	—

^aError from estimation procedure only.

^bScaling factor (%) that is multiplied to the reference OH field.

^cScaling factor (%) that is multiplied to the 1970–1978 emissions.

Table 2. Optimization of OH in 5-Year Periods

Parameter	Value	σ^a
1951–1980 ^b	–11.2	0.6
1981–1985	–5.6	0.4
1986–1990	–2.4	0.4
1991–1995	–4.8	0.3
1996–2000	–12.2	0.1
ΔE^c	0.0	0.2
ϵ	0.997	0.003
J/N	0.99	—

^aError from estimation procedure only.

^bScaling factor (%) that is multiplied to the reference OH field.

^cScaling factor (%) that is multiplied to the 1970–1978 emissions.

Table 3. Optimization of OH According to Eq. 4

Parameter	Value	σ^a
a^b	-7.4	0.3
b	-0.14	0.02
c	-0.198	0.004
ΔE^c	-0.3	0.2
ϵ	0.994	0.003
J/N	1.01	—

^aError from estimation procedure only.

^bParameters of Eq 4.

^cScaling factor (%) that is multiplied to the 1970–1978 emissions.

Table 4. Hemispheric OH Optimization

According to Eq. 4

Parameter	Value	σ^a
a_N^b	-18.0	0.6
a_S	0.1	0.5
b	0.12	0.03
c	-0.162	0.005
ΔE^c	0.2	0.2
ϵ	1.023	0.003
J/N	0.89	—

^aError from estimation procedure only.^bParameters of Eq 4.^cScaling factor (%) that is multiplied to the 1970–1978 emissions.

Table 5. Optimization of the Emissions in 3-Year Periods

Parameter	Value ($\pm\sigma$) ^a	Emitted ^b (Gg)	Excess ^c (Gg)
1977–1979 ^d	+6.1±0.9	1485.3	+90.1
1980–1982	+0.6±0.5	1609.5	+9.2
1983–1985	−1.0±0.5	1714.1	−16.8
1986–1988	−1.8±0.5	1819.3	−34.3
1989–1991	−3.8±0.5	2043.6	−77.8
1992–1994	+0.3±0.6	1256.3	+3.6
1995–1997	+2.2±0.8	367.3	+8.1
1998–2000	+82.4±2.9	65.3	+53.8
ϵ	0.999±0.005	—	—
J/N	0.90	—	—

^aError from estimation procedure only.

^bTotal emissions is the 3-year period.

^cExcess that corresponds to the optimized scaling factors.

^dScaling factor (%) multiplied to the emissions in this period.

Table A1. Tropospheric Lifetimes in TM3 and MOGUNTIA

Year	OH ^a (yr)		Strat ^b (yr)		Ocean ^c (yr)		Total ^d (yr)	
	TM3	MOG	TM3	MOG	TM3	MOG	TM3	MOG
1980	5.47	5.36	34.1	34.3	78.5	82.9	4.45	4.39
1985	5.47	5.37	36.2	36.6	78.3	82.7	4.48	4.43
1990	5.47	5.37	36.3	36.8	78.2	82.5	4.48	4.44
1995	5.48	5.40	46.8	45.1	78.0	82.6	4.61	4.55
2000	5.48	5.41	58.2	58.4	77.7	82.3	4.71	4.67

^aTropospheric MCF burden divided by tropospheric OH oxidation.

^bTropospheric MCF burden divided by loss to the stratosphere.

^cTropospheric MCF burden divided by ocean uptake.

^dTropospheric MCF burden divided by the total loss.